



NRL/MR/5524--15-9576

Distributed Transmitter Localization by Power Difference of Arrival (PDOA) on a Network of GNU Radio Sensors

ANDREW ROBERTSON

SASTRY KOMPELLA

JOE MOLNAR

*Networks and Communications Branch
Information Technology Division*

FRANK FU

*KEYW Corporation
Hanover, Maryland*

MATTHEW DILLON

*Catholic University of America
Washington, D.C.*

DMITRI PERKINS

*University of Louisiana at Lafayette
Lafayette, Louisiana*

February 3, 2015

Approved for public release; distribution is unlimited.

REPORT DOCUMENTATION PAGE

Form Approved
OMB No. 0704-0188

Public reporting burden for this collection of information is estimated to average 1 hour per response, including the time for reviewing instructions, searching existing data sources, gathering and maintaining the data needed, and completing and reviewing this collection of information. Send comments regarding this burden estimate or any other aspect of this collection of information, including suggestions for reducing this burden to Department of Defense, Washington Headquarters Services, Directorate for Information Operations and Reports (0704-0188), 1215 Jefferson Davis Highway, Suite 1204, Arlington, VA 22202-4302. Respondents should be aware that notwithstanding any other provision of law, no person shall be subject to any penalty for failing to comply with a collection of information if it does not display a currently valid OMB control number. **PLEASE DO NOT RETURN YOUR FORM TO THE ABOVE ADDRESS.**

1. REPORT DATE (DD-MM-YYYY) 03-02-2015			2. REPORT TYPE Memorandum Report		3. DATES COVERED (From - To)	
4. TITLE AND SUBTITLE Distributed Transmitter Localization by Power Difference of Arrival (PDOA) on a Network of GNU Radio Sensors					5a. CONTRACT NUMBER	
					5b. GRANT NUMBER	
					5c. PROGRAM ELEMENT NUMBER	
6. AUTHOR(S) Andrew Robertson, Sastry Kompella, Joe Molnar, Frank Fu, ¹ Matthew Dillon, ² and Dmitri Perkins ³					5d. PROJECT NUMBER	
					5e. TASK NUMBER	
					5f. WORK UNIT NUMBER	
7. PERFORMING ORGANIZATION NAME(S) AND ADDRESS(ES) Naval Research Laboratory, Code 5524 4555 Overlook Avenue, SW Washington, DC 20375-5320					8. PERFORMING ORGANIZATION REPORT NUMBER NRL/MR/5524--15-9576	
9. SPONSORING / MONITORING AGENCY NAME(S) AND ADDRESS(ES) Naval Research Laboratory, Code 5524 4555 Overlook Avenue, SW Washington, DC 20375-5320					10. SPONSOR / MONITOR'S ACRONYM(S)	
					11. SPONSOR / MONITOR'S REPORT NUMBER(S)	
12. DISTRIBUTION / AVAILABILITY STATEMENT Approved for public release; distribution is unlimited.						
13. SUPPLEMENTARY NOTES ¹ KEYW Corporation, 7740 Milestone Pkwy, Suite 400, Hanover, MD 21076 ² Catholic University of America, 620 Michigan Avenue, NE, Washington, DC 20064 ³ University of Louisiana at Lafayette, 104 E University Avenue, Lafayette, LA 70504						
14. ABSTRACT The localization of an RF transmitter by a distributed set of RF receivers has important application to the Navy. We report the results of a transmitter localization experiment done at the Naval Research Laboratory. A distributed sensor network was implemented on GNU radio and field-tested. The network locates target emitters using differences in received powers between sensors. We discuss the localization algorithm and the likely sources of error associated with it. We review simulated and experimental results consistent with our interpretations of the error sources, and we suggest methods for dealing with these errors in future iterations of the sensor network.						
15. SUBJECT TERMS						
16. SECURITY CLASSIFICATION OF:			17. LIMITATION OF ABSTRACT Unclassified Unlimited	18. NUMBER OF PAGES 14	19a. NAME OF RESPONSIBLE PERSON Andrew Robertson	
a. REPORT Unclassified Unlimited	b. ABSTRACT Unclassified Unlimited	c. THIS PAGE Unclassified Unlimited			19b. TELEPHONE NUMBER (include area code) (202) 767-3262	

CONTENTS

1. BACKGROUND	1
2. MODEL OF TRANSMITTER LOCALIZATION.....	2
3. EXPERIMENTAL AND SIMULATED RESULTS.....	6
4. CONCLUSIONS AND FUTURE WORK	10
ACKNOWLEDGMENTS	11
REFERENCES	11

DISTRIBUTED TRANSMITTER LOCALIZATION BY POWER DIFFERENCE OF ARRIVAL (PDOA) ON A NETWORK OF GNU RADIO SENSORS

1. BACKGROUND

Geolocation of radio frequency emitters is one of the fundamental capabilities of spectrum situational awareness and provides a variety of uses in military communications when working in tactical environments. Knowing the location and power level of a radio frequency emitter provides useful information situational awareness in DSA radio technology. The big picture is to design a hierarchical spectrum sensing architecture. Low-level communication nodes are responsible for sensing the radio spectrum and reporting relevant data while the intermediate level node, also known as the correlation engine, is responsible for taking the reports from low-level nodes and providing spectrum situational awareness. This clustering of functionality ultimately reduces data overhead as sensing reports do not need to travel all the way up a network hierarchy before being processed and reported back down. Most of the processing occurs at the intermediate level in small sensor clusters.

The accuracy of a transmitter localization methods depends on what RF information the sensors can collect about the target emitter and the channel through which that information propagates. If the sensors have very accurate synchronized clocks, they can estimate the difference in time that a target transmission takes to get to each receiver. Location by means of this information is called *Time Difference of Arrival* (TDOA), and it requires robust clock hardware and network overhead for synchronization [1, 2]. If the radios can tell the direction from which a target signal comes, it can analyze the angle of arrival (AOA) to localize the transmitter [1, 3]. Just as with TDOA, this requires more robust hardware: this time in the form of directional antennas. The simplest algorithm requiring the least hardware investment is to localize by received signal strength [1, 4, 5]. Because our intended scenario of low-complexity distributed sensors has stringent hardware requirements, this is the strategy we employ in our network. The price we pay for the simplicity is lower accuracy in target emitter location estimates.

In this work, we describe the construction of a sensor network of Ettus USRP software defined radios running the GNU radio software suite. These sensors measure the received power from a target emitter at an unknown location and with an unknown transmission power. They report their measurements to a fusion center node that performs the localization algorithm. The emitter localization is based on the power-difference of arrival (PDOA) algorithm in [6]. The algorithm creates a set of circular loci of possible emitter locations based on the power-difference between sensors' received target signal power. The intersections of all pairs of circles are calculated. The algorithm then performs a grid-search in which the cell with the largest intersection density is chosen as the estimated emitter location. We execute this protocol many times under varying conditions (emitter location and number of sensors) both in simulation and in a field-test on the NRL mall. We report the results of these tests, and we discuss the error sources particular with our protocol. Our results indicate that the main source of error is geometric having to do with the way potential emitter loci are calculated. This source is exacerbated by non-idealities of the channel. We discuss potential mitigations strategies that will appear in future iterations of our sensor network.

2. MODEL OF TRANSMITTER LOCALIZATION

Consider a number of transceivers distributed spatially over some area of operations (AO). Their goal is to locate a target emitter transmitting at a constant but unknown power P_T from some unknown location denoted (x_T, y_T) . All of the sensors as well as the emitter are assumed to be at the same altitude, so the sensors are tasked only with finding the emitter's latitude and longitude. They will do this by measuring the power received from the target emitter, and leveraging the relationship between path loss and distance.

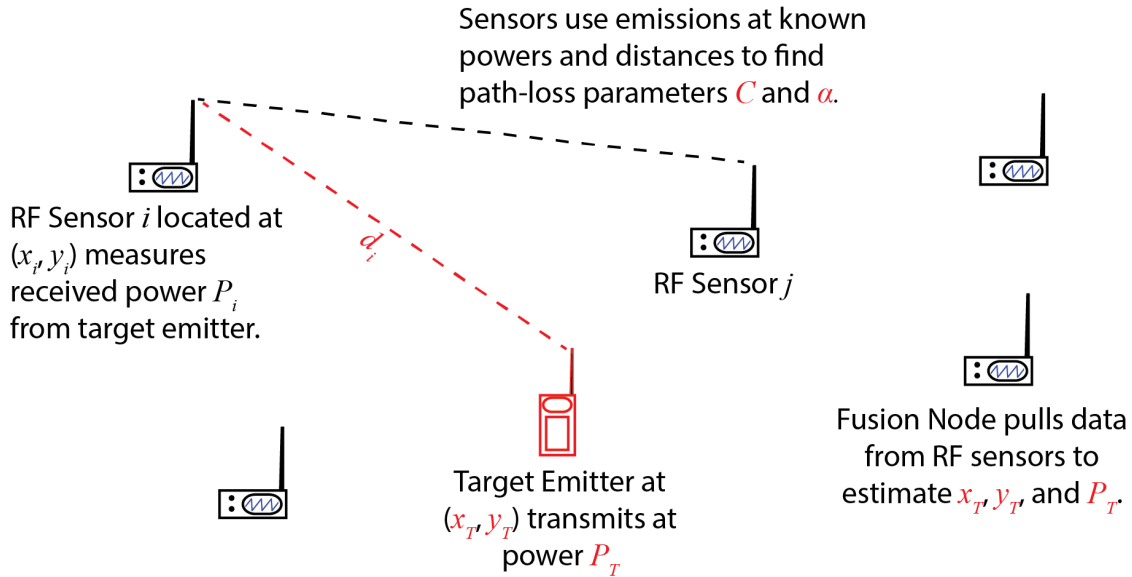


Fig. 1 — An abstraction of our system. Quantities in red are initially unknown and must be estimated.

We model path loss as an exponential function of the distance d_i between the target emitter and the receiving sensor. That is, the received signal power is proportional to $d_i^{-\alpha}$, where α is an initially unknown path loss exponent that ranges between 2 and 6 as described in [7]. The constant of proportionality C is also unknown, so both C and α will have to be estimated during sensor network initialization. Once this is done, we will have a system of N equations of the form $P_i = \frac{C}{|d_i|^\alpha} P_T$. Our experimental work is easier if we quote power measurements in decibels, so we define $\hat{P}_i = 10 \log_{10} P_i$, $\hat{C}_i = 10 \log_{10} C$, and $\hat{P}_T = 10 \log_{10} P_T$ to arrive at the following relation.

$$\hat{P}_i = \hat{C}_i - 10\alpha \log(d_i) + \hat{P}_T \quad (1)$$

The sensors use an out-of-band frequency to wirelessly communicate their received power measurements $\{\hat{P}_i\}_{i=1}^N$ to the fusion center. The fusion center then uses the grid-density based power difference on arrival (PDOA) algorithm in [6] to estimate the location of the target emitter. The PDOA algorithm begins with the path loss model in Eq. (1). With the list of received power measurements, the fusion center can calculate

the difference between the received power on any two sensors canceling out the \hat{C} and \hat{P}_T terms.

$$\hat{P}_i - \hat{P}_j = 10\alpha \log \left(\frac{d_j}{d_i} \right) \quad (2)$$

Thus with an estimate of the path loss exponent α , the fusion center can use the differences in received powers to form an estimate $q_{ij} \approx \frac{d_i}{d_j}$ of sensor-to-emitter distances. Let us assume that $q_{ij} = 10^{(\hat{P}_i - \hat{P}_j)/10\alpha}$ has been calculated by means of this method for all possible sensors i, j . Let us further assume that there are three or more sensors in different locations. As shown in Fig. (1), the power measurement from a sensor i can be used to constrain the emitter location (x_T, y_T) to lie on a circle of radius d_i centered at the point (x_i, y_i) . Unfortunately finding the radius of this circle requires knowing P_T . With the measurements from two sensors, we can find the *ratio* of the distances from the two sensors to the target without knowing P_T . This requires less information, and the price is that every pair of sensor measurements constrains the emitter location to be on a *set* of points: the Circle of Apollonius [8].

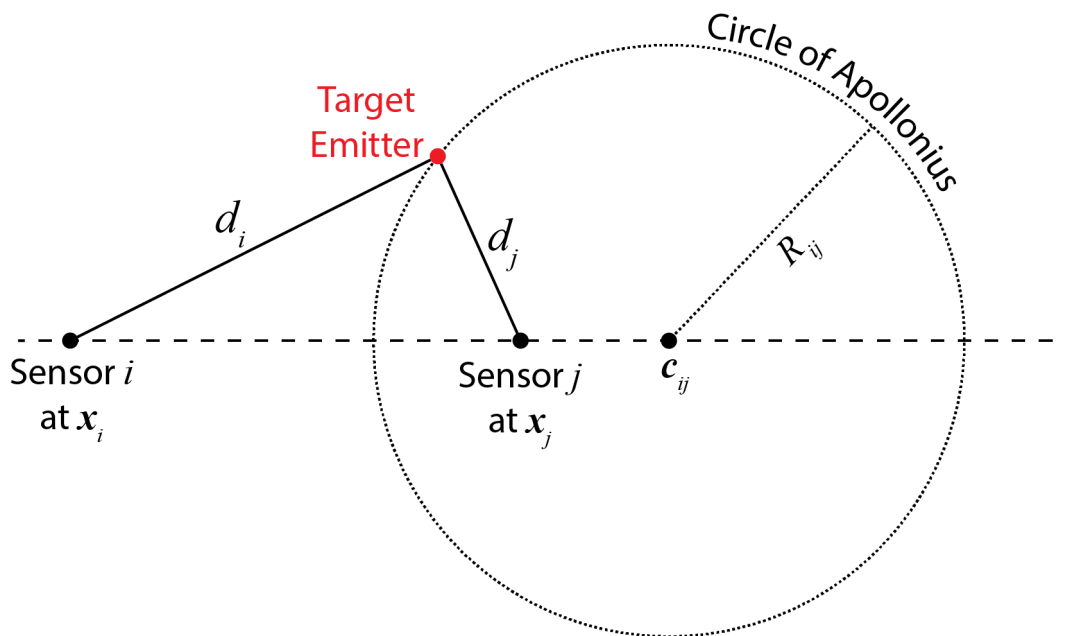


Fig. 2 — The Circle of Apollonius. Given a ratio of distances q_{ij} to the target emitter, each pair of sensors i and j defines a circle of points (see Eq. (3)) on which the target emitter could be located.

Given two points and a positive constant not equal to 1, the set of points having distances to the two foci in ratio equal to the constant has been known to be a circle since the time of Apollonius of Perga. The concept of the circle of Apollonius is depicted in Fig. (2). In the framework of our sensor network, each pair of sensors i and j defines a circle that is the set of points for which the distance to \mathbf{x}_i and the distance to

\mathbf{x}_j have the same constant ratio q_{ij} . The center and radius of the circle are given by:

$$\begin{aligned} \mathbf{C}_{ij} &= \frac{q_{ij}^2 \mathbf{x}_j - \mathbf{x}_i}{q_{ij}^2 - 1} \\ R_{ij} &= q_{ij} \frac{|\mathbf{x}_j - \mathbf{x}_i|}{|q_{ij}^2 - 1|} \end{aligned} \quad (3)$$

Because q_{ij} has been estimated using Eq. (2) from received powers and is known to approximate d_i/d_j , the target location \mathbf{x}_T is constrained to lie approximately on the circle defined by Eq. (3). Notice that the quantities in Eq. (3) do not depend explicitly on P_T . However there is a danger of divergence when the $q_{ij} = 1$. This corresponds to the case where the target is equidistant from the two sensors in question. In this case the set of points that are equidistant from two points is not a circle at all. It is a straight line: the perpendicular bisector between the two sensor locations. This line can be thought of as a ‘‘circle’’ with infinite radius centered at infinity, but it is more prudent for future versions of the localization algorithm to recognize this edge case and model the locus as a line.

Assume R_{ij} and \mathbf{C}_{ij} to be calculated for each pair of sensors resulting in $N(N-1)/2$ circles. For power measurements from at least four non-concentric sensors in a perfect channel, every circle would intersect at a single point: the target emitter location. With noisy measurements, there will not be a point common to all circles. However if the channel does not distort the measurements of q_{ij} too much, the distribution of intersection points should still be highest near the target emitter. A grid-based algorithm for finding the peak of the intersection point distribution was presented in [6].

The algorithm begins by calculating the intersection points between every pair of circles. In the event that there are no intersections between a pair of circles, the algorithm uses the midpoint of the line segment joining the two centers. Assume there to be an intersection between a first circle defined by $\mathbf{C}_{ij} = (x_1, y_1)$ and $R_{ij} = r_1$ and a second circle defined by $\mathbf{C}_{mn} = (x_2, y_2)$ and $R_{mn} = r_2$. There will be two points of intersection given by the following equation [6, 9].

$$\begin{aligned} x_{12} &= x_1 + \frac{a}{d} (x_2 - x_1) \pm \frac{b}{d} (y_2 - y_1) \\ y_{12} &= y_1 + \frac{a}{d} (y_2 - y_1) \mp \frac{b}{d} (x_2 - x_1) \end{aligned} \quad (4)$$

where $d = |\mathbf{C}_{ij} - \mathbf{C}_{mn}|$ is the distance between the centers of the two circles and the constants a and b have the following forms.

$$\begin{aligned} a &= (r_1^2 - r_2^2 + d^2) / (2d) \\ b &= \sqrt{|r_1^2 - a^2|} \end{aligned} \quad (5)$$

Because Eq. (4) defines two solutions, there are two possibilities for the target emitter’s location. Each pair of sensors produces two intersection points: one that is close to the target emitter and one *false location* for the emitter. Because the emitter is located at the unique intersection of *all* circles in a perfect channel, one hopes that the distribution of intersection points will be peaked near the emitters location in a noisy distorted

channel. With some caveats having to do with sensor geometry (which we will discuss later), this is indeed the case for weak noise and distortion. A grid search algorithm can be used to find the peak in the spatial intersection distribution and estimate the target location.

Our grid search algorithm overlays a configurable number of cells on the area of interest once all of the intersections are determined. In our experiment, a 4x4 grid was used for an approximately 100-meter by 50-meter area. The goal is for the cells to be large enough that the intersections corresponding to the emitter's true location fall easily into one cell but small enough such that localization of the emitter to a single cell meets the desired spatial resolution. Clearly it would be worthless to localize the target emitter into a cell that is the size of the entire area of interest. Once the grid is created, a search algorithm finds the grid cell with the highest number of intersections. In the event that two or more grid cells have the same number of intersections, the number of intersections in all adjacent grid cells break the tie. The grid cell with the most intersections adjacent to it is considered the highest density cell. In the unlikely event that there is still a tie between two or more cells, the midpoint between the two cells' centers is taken as the estimated emitter location. Once the highest density cell is selected, the intersection locations are averaged to find the final estimate of the target emitter's location. This last calculation is similar to the computation of a center of mass for a number of point masses of equal weight.

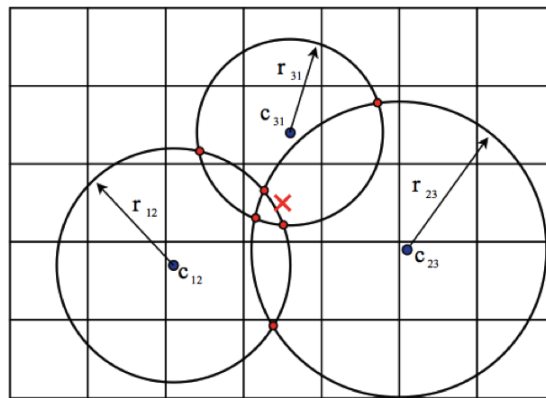


Fig. 3 — The grid search algorithm concludes that the cell with the highest number of intersection points contains the target emitter. It then averages the locations of the intersections within that cell to estimate the location of the emitter.

Figure (3) illustrates the grid-density algorithm for a three-sensor case. Notice how each pair of circles yields a true point in the cell with an “X” and a false point in some other cell. A network of N sensors in a low-noise channel produces $N(N-1)$ intersection points. The cells should optimally be sized so that the true points all fall within a cell while the false points reliably fall outside that cell. For each pair of sensors, the false and true points will be separated by a distance of $2b$ where b is related to the circle radii and centers via Eq. (5). It is reasonable to expect that there is some optimal cell size related to the geometry of the sensor network, but this aspect has yet to be explored.

3. EXPERIMENTAL AND SIMULATED RESULTS

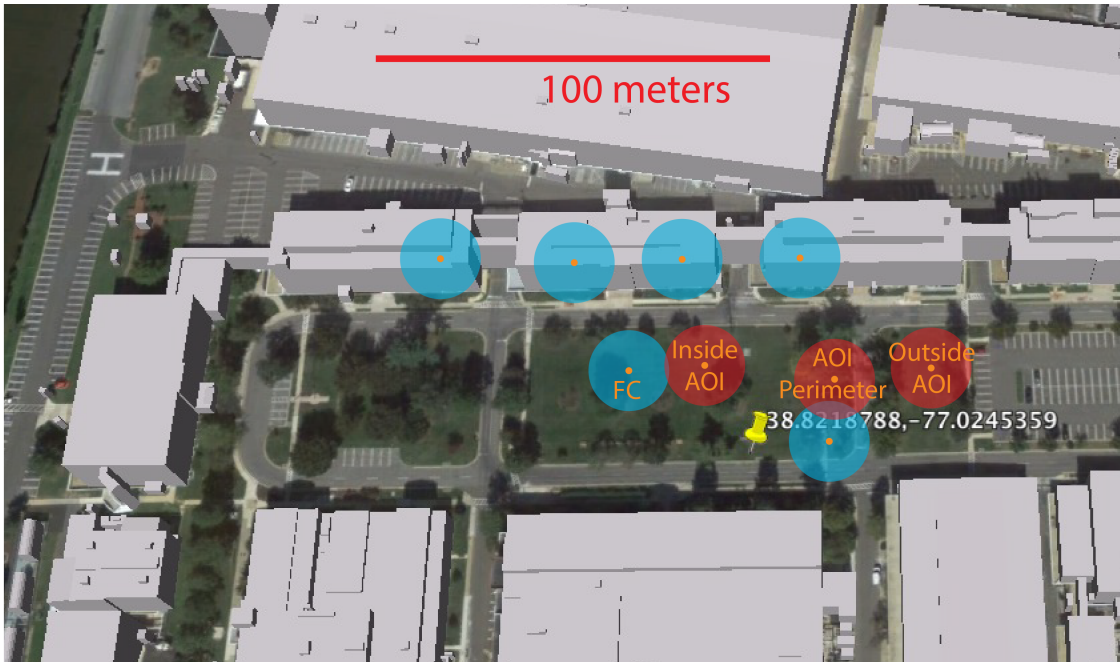


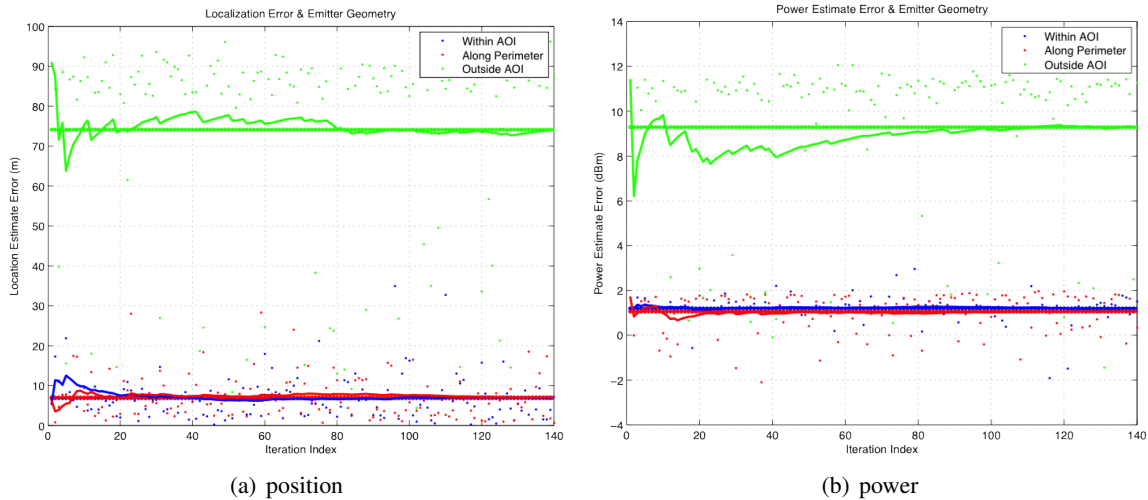
Fig. 4 — The sensors and target placements during our experiment on the NRL mall.

In our experiment, five software defined radios (Ettus USRP's) were placed at locations around the mall at the Naval Research Laboratory in Washington, D.C as shown in Fig. (4). A target emitter was placed at one of three locations on the grounds. These locations were chosen to be within the perimeter, on the perimeter, and outside the perimeter of the area of interest (AOI). Even though the locations are reasonably close together, they yield different error performances due to the non-linear way in which errors depend on sensor and emitter geometry. The emitter transmitted a sinusoid at 903 MHz with a constant power unknown to the sensors. For each location of the target emitter, the sensors would record their received powers at 903 MHz and send that information to a fusion center once every 5 seconds. The sensors would also send their GPS coordinates. With the received powers, the fusion center would then implement the PDOA algorithm described in Chapter 2 to estimate the emitter location. Finally, the emitter would use the received power data and the location estimate to produce a transmitter power estimate. It would then send these estimates back to the distributed sensors. This process was iterated many times and the estimates were logged.

Before the experiment began, we needed to estimate the path loss parameter α in Eq. (2). A preliminary field measurement was conducted wherein a single USRP was taken out to the field and placed in six different locations at increasing distance from the target emitter. Measurements of power at 903 MHz were taken with a spectrum analyzer program on the USRP and a range finder was used to measure the distance between the emitter and sensor locations. With this data the model in Eq. (1) can be linearized where $\log(d_i)$ is the independent variable and $\hat{P}_i - \hat{P}_T$ is the dependent variable. The slope of the line representing the relationship between these variables is the path loss constant, α . The y-intercept is the normalization

constant, C . After the preliminary field measurements were taken to determine the path loss parameters, the results were linearized and plotted. The best fit line was found to be $\alpha = 2.4282$ and $C = 0.003992$.

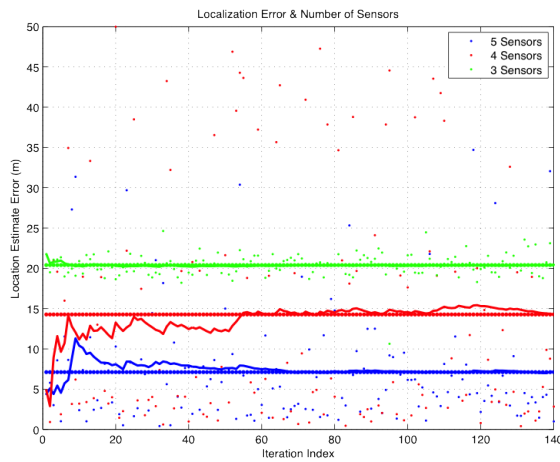
The field-test described in Fig. (4) was also simulated for verification and repeatability purposes. To mimic the effect of a noisy channel with shadowing and fading, a random Gaussian term was added to the path loss model in Eq. (2). Within the simulation, we can see how the sensor-emitter geometry and the number of sensors used affects the localization and transmission power errors. We also see the effect of averaging many runs of produce a less noisy estimate. However noise is not the main source of error, and we will find that systematic errors that cannot be averaged away are likely due to sensor geometry. The time it takes for the error to converge to the overall mean error tells us something about the spread in our location estimates. In our experiments and simulations, 140 iterations of the communications program and localization algorithm were executed for each target emitter location.



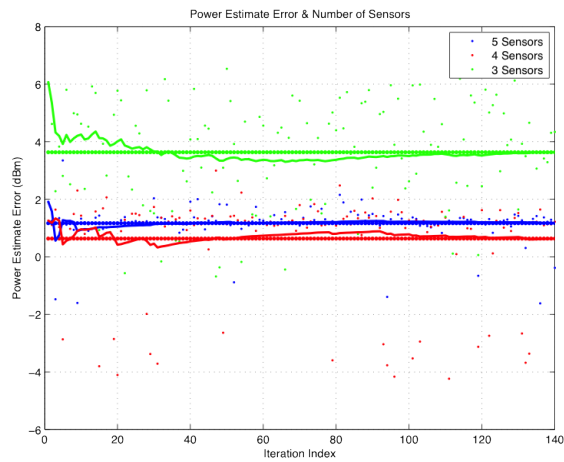
In figures (5(a)) and (5(b)) we find the results of simulations across the space of possible target emitter locations. For the case of the emitter being within the sensor network area, the algorithm better estimated emitter location with an error margin less than 10 meters. The results for when the emitter is along the perimeter were almost the same. However the case where the emitter is taken outside the network area of interest is surprising. The results are much poorer (by nearly an order of magnitude) despite the target emitter having been moved by less than 40 meters. This can be partly explained as far-away sensors not picking up the emitter power as easily. Thus the measurements of the received power are noisier, and thus the estimated distance ratios q_{ij} are noisier. However note that the error distribution in Fig. (5(a)) is bimodal. There is a common component with an average error around 80 meters from the actual target, but there is also a rarer component with an average error closer to 30 meters. If one were to draw out the Apollonian circles for the configuration as was done for Fig. (3), one would see the intersection points constantly jiggling from one iteration of the communication protocol to the next. This is because the noisy measurements of the target's received power make the intersection points of these circles move in a stochastic fashion. One can envision a situation wherein two grid cells had roughly the same high number of intersections.

Random fluctuations would sometimes give one cell more intersections than the other. Thus, the grid search algorithm would be hopping between these two cells as each alternated position as the one with the highest number of intersections. In the case of the out-of-AOI simulations in Fig. (5(a)), it seems that the cell that is further from the target emitter randomly tends to have more intersections in it more often than the one that is actually closer. This results in a larger error spread and consequently a larger convergence time as well. In the future, we hope to add simple controls that will let the fusion center know when its estimates are hopping between two cells sequentially. Perhaps this will suggest a way to tell which of the cells has lower error associated with it.

From figures (5(g)) and (5(h)) below, it is shown that the number of sensors also has a significant impact on the performance of the algorithm. The error was observed to be smaller when more sensors are added. However, according to the simulation results from [6], the effect of the number of sensors on the algorithm becomes negligible above a certain number of sensors. Due to limited resources, only a maximum of five sensors were used for this field test. One easily sees that the error spread and the convergence time is lower in experiments with fewer sensors. This is a little surprising because it is often taken for granted that more sensors should mean a shorter convergence times because noise is averaged away faster. Of course this is only true when noise is the primary source of errors. In our case, one could interpret more sensors as meaning more circle intersections which are fluctuating in location between communication iterations. The distribution of intersections is flatter as any given cell has a higher average number of intersections in it, and the grid search algorithm picks an incorrect cell with higher probability. It is likely that the search algorithm is picking uniformly from a small number of cells that have comparably high and fluctuating numbers of intersections. This is the source of the multi-modality of the error distributions.

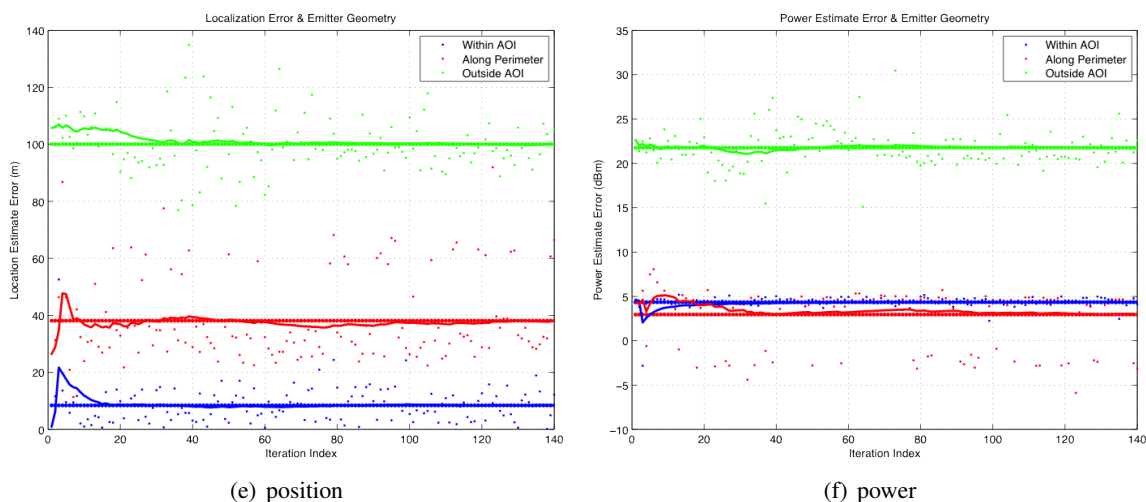


(c) position



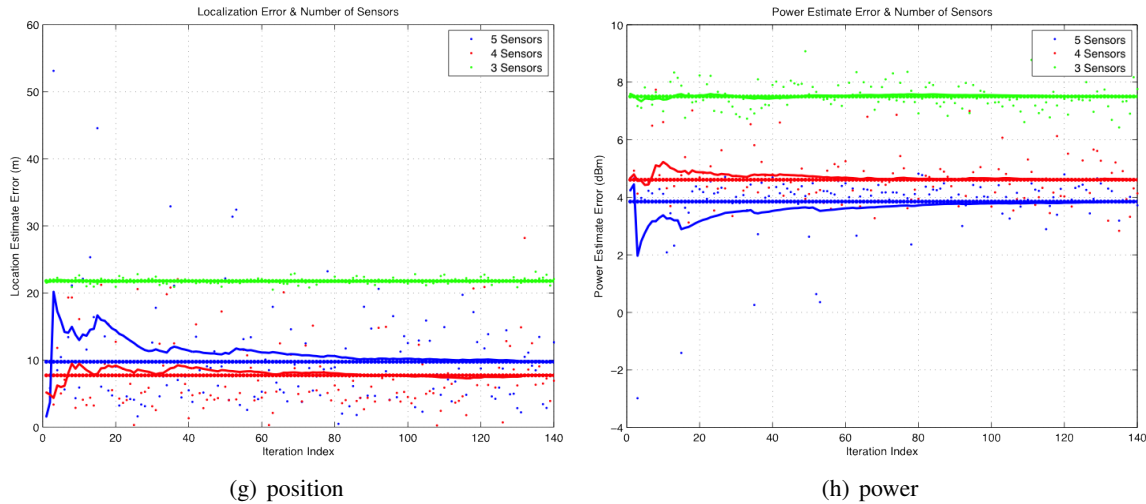
(d) power

With a feel for the types of results we can expect from our simulations, we can now consider the actual performance of our sensor network in the field-test on the NRL mall. In figures (5(e)) and (5(f)), the field-test results show a trend in error similar to the simulation results when the emitter is moved to different locations. The time-averaged errors are greater in magnitude for the experiment compared to the simulation, but we can attribute this to the non-trivial channels that the radios face in the real world. The short convergence times and error spreads indicate again that noise is not the primary source of error. Rather the multi-modality of the error distribution suggests a geometric reason as we saw in the simulations though this error source can certainly be exacerbated by noise. We still find the worst performance when the emitter is outside the AOI and comparatively better performance when the emitter is on or within the AOI perimeter. Note that the power estimates are noisier for runs outside the AOI. We understand this from simulation as the sensors having noisier measurements of received power due to more distance-based fading. Note also that the modality of the error distribution in power matches that of the error distribution in location. We expect this to be true because the the location estimate is input for the power estimation algorithm. Any errors in emitter location should be recapitulated in emitter power estimates.



In figures (5(g)) and (5(h)), we find the field test results over the space of sensor network size. These results largely agree with our simulations even regarding the surprising effects. We again see from the convergence time and error spread for the three sensor case counterintuitively has the lowest location estimate variance. While the error is highest for these cases, one would expect to see at least bimodality in the error distribution. This is because of a well-known geometric fact that *any* emitter location and power will produce the same received power at any three receivers as some other emitter at a different location and power. More concretely there should be an unavoidable false target location between which the search algorithm should be switching from iteration to iteration. This is an artifact of the theorem that any three sensors are concentric. It is possible that these false points do in fact exist but that they are outside the AOI. This would account for the absence of bimodality in the 3-sensor runs, but more work will be necessary to verify this. Also note that the runs with four sensors had lower average error than the runs with five. This may be coincidence of the sensor's placement, but it is not unreasonable to think that there is an optimal

number or density of sensors such that intersection distribution is sufficiently peaked; enough sensors so that high density cells can be distinguished from low density cells, but not so many that the distribution of intersections across cells flattens.



4. CONCLUSIONS AND FUTURE WORK

Over the course of this experiment, we demonstrated a distributed sensor network capable of locating an emitter with an unknown transmission power. The network has been simulated in Matlab and implemented on GNU Radio transceivers. The network uses a simple algorithm that locates the transmitter by analyzing the differences in power received at a given frequency by sensors at different known locations. The price paid for the simplicity of the algorithm is the existence of a number of error modes discussed in the previous section. Our results indicate that errors primarily arise from two sources: the multiple intersection points of the sensors' Apollonian circles and non-idealities of the channel i.e. departures of the real channel from Eq. (1). Despite these errors, the sensor network performed reasonably (with accuracy in the tens of meters) in a field test conducted on the NRL mall.

Future work will focus primarily on mitigating the aforementioned error sources. Corrections to the algorithm should include a routine that models the locus of potential emitter locations as a perpendicular bisector of line segment connecting the sensors when they calculate very similar received powers. This will likely perform better than modeling the locus as an Apollonian circle because it will avoid the divergence in the denominators of Eq. (3). To mitigate the effects of the ambiguity of circle intersections, an upgraded algorithm could optimize some cost function depending on *all* sensor received powers over the space of possible emitter locations rather than multiple pairs of measurements. We expect that this would reduce the propensity of our algorithm to "hop" between two different choice locations. The non-ideal channel is the other big error source to be mollified. Some ground can be gained by having the sensors calibrate themselves and measure α in Eq. (1) before each sensing period. Indeed we have started work on a protocol that does

this, but it will not help with more complex channels including multipath and shadowing. For these, more advanced channel modeling techniques must be discovered.

In addition to making the sensor network more robust to errors, we plan to add functionality to it. The network presently works under the assumption that it knows the emission frequency of its target. It also assumes that *only* the target emitter is operating at the frequency of interest. Future iterations will scan the band for signals to separate in time, frequency, and modulation. The network will then classify them into signals of interest and other emissions before attempting to locate the interesting ones. Work will also focus on executing the information processing as well as the sensing in a distributed fashion. That is to say that future iterations of this sensor network will ideally have no dedicated fusion centers. All nodes will be capable of functioning as the fusion center, and they will execute distributed processing to reduce communication overhead and mitigate single points of failure.

ACKNOWLEDGMENTS

The NRL team wishes to acknowledge the collaboration with the office of the Secretary of Defense (OSD). We would especially like to thank Dr. Syed Shah (OSD) and the Joint Tactical Edge Networks (JTEN) working groups for enabling and supporting our experiments.

REFERENCES

1. I. Jami, "Comparison of methods of locating and tracking cellular mobiles," *IET Conference Proceedings* pp. 1–1(1) (January 1999), URL http://digital-library.theiet.org/content/conferences/10.1049/ic_19990238.
2. K. Krizman, T. Biedka, and T. Rappaport, "Wireless position location: fundamentals, implementation strategies, and sources of error," in *Vehicular Technology Conference, 1997, IEEE 47th*, volume 2, pp. 919–923 vol.2 (May 1997), doi: 10.1109/VETEC.1997.600463.
3. N. Patwari, J. Ash, S. Kyperountas, A. Hero, R. Moses, and N. Correal, "Locating the nodes: cooperative localization in wireless sensor networks," *Signal Processing Magazine, IEEE* **22**(4), 54–69 (July 2005), ISSN 1053-5888, doi: 10.1109/MSP.2005.1458287.
4. P. Bergamo and G. Mazzini, "Localization in sensor networks with fading and mobility," in *Personal, Indoor and Mobile Radio Communications, 2002. The 13th IEEE International Symposium on*, volume 2, pp. 750–754 vol.2 (Sept 2002), doi: 10.1109/PIMRC.2002.1047322.
5. G. Mao, B. Fidan, and B. D. Anderson, "Wireless sensor network localization techniques," *Computer Networks* **51**(10), 2529 – 2553 (2007), ISSN 1389-1286, doi: <http://dx.doi.org/10.1016/j.comnet.2006.11.018>, URL <http://www.sciencedirect.com/science/article/pii/S1389128606003227>.
6. S. Guo, B. Jackson, S. Wang, R. Inkol, and W. Arnold, "A novel density-based geolocation algorithm for a noncooperative radio emitter using power difference of arrival," in *SPIE Defense, Security, and Sensing*, pp. 80610E–80610E (International Society for Optics and Photonics, 2011).
7. B. R. Jackson, S. Wang, and R. Inkol, "Emitter Geolocation estimation using power difference of arrival. An algorithm comparison for non-cooperative emitters," rept., Defence R&D Canada - Ottawa, DRDC Ottawa (May 2011).

-
8. J. Cox and M. B. Partensky, “Spatial localization problem and the circle of Apollonius,” *arXiv preprint physics/0701146* (2007).
 9. E. W. Weisstein, “Circle-circle intersection. From MathWorld—A Wolfram Web Resource” (2014), URL <http://mathworld.wolfram.com/Circle-CircleIntersection.html>, Last visited on 2014-09-23.